Broken symmetry and competing orders in Weyl semimetal interfaces

Ritajit Kundu, H. A. Fertig, and Arijit Kundu

Broken symmetry and competing orders in Weyl semimetal interfaces

Ritajit Kundu,[1] H.A. Fertig,[2, 3] and Arijit Kundu[1]

[1]*Department of Physics, Indian Institute of Technology Kanpur, Kanpur 208016, India*
[2]*Department of Physics, Indiana University, Bloomington, IN 47405*
[3]*Quantum Science and Engineering Center, Indiana University, Bloomington, IN, 47408*

We consider interaction-induced broken symmetry states of two Weyl semimetal surfaces with multiple Fermi-arc (FA) states. In the presence of inter- and intra-surface Coulomb interactions, multiple broken symmetries may emerge which coexist and/or compete with one another. Interlayer exciton condensates involving different FA flavors are shown to form, with amplitudes determined by the strength of interactions and the degree of nesting among the arcs. For FA pairs which are well-separated in momentum with strong nesting, the resulting state is a particle-hole analog of a Fulde–Ferrell–Larkin–Ovchinnikov (FFLO) superconductor. Intralayer interactions moreover induce charge density wave (CDW) ordering, so that the most general state of the system is a supersolid. These orderings in principle carry signatures in non-linear behavior and narrow band noise in Coulomb drag transport measurements.

INTRODUCTION

Weyl semimetals (WSMs) are three dimensional topological systems with an even number of band-touching points (Weyl nodes) in their bulk band-structure [1, 2]. Because of their intrinsic topology, non-overlapping surface projections of Weyl nodes connect endpoints of disjoint Fermi surface sections known as Fermi-arcs (FAs). FAs host surface states that disperse in a quasi-one-dimensional manner. There are extensive ongoing efforts to identify material candidates for WSMs, both theoretically and experimentally. Examples of such materials include TaAs [3], NbAs [4] and, more recently, CoSi, $Co_3Sn_2S_2$, for which FA modes have been identified in ARPES and quasiparticle interference experiments [5–7]. Although they may lack topological protections, FAs of Dirac semimetals, such as Na_3Bi and Cd_3As_2, have been also identified in recent times [8–13].

Interactions may introduce interesting physics in WSMs, involving either or both the bulk states and the FA states. For example, collective excitations confined to the surfaces are expected to be supported [14–23], as are bulk excitonic modes and density-wave instabilities [24, 25], among other possibilities [2]. Interesting effects also occur when two Weyl systems are brought together. For example, intricate reconstruction of FA geometry can sometimes occur due to inter-surface tunneling [26–28]. In the absence of tunneling, inter-surface Coulomb interactions may induce coherent particle-hole processes involving FA states of both surfaces, leading to new collective excitations and broken symmetry states. This is the subject of our study. As explained below, we find that a number of symmetries may break in such systems: the local gauge symmetry, which conserves particle number of each layer, due to inter-surface exciton condensation [29], in similarity with other bi-layer systems, such as in graphene [30–32]; translational symmetry, through the formation of charge-density-wave (CDW) order; and, in each case, coherences may set in among different pairs
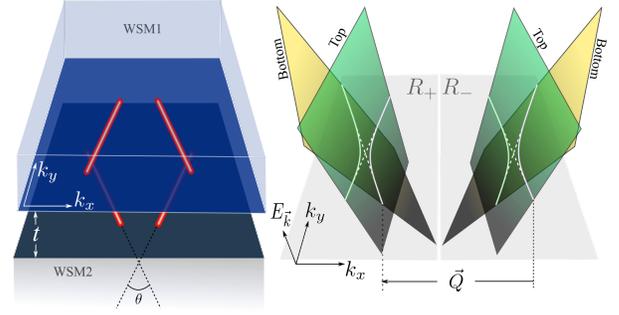
FIG. 1. Left: Two WSM surfaces with FAs indicated in the surface Brillouin zones, which are separated by a dielectric slab of thickness t. Two FAs reside on each surface with an angle θ between them. Right: Dispersions of the FAs. White dashed lines indicate Fermi surfaces without interactions. With interactions the Fermi surfaces distort to the solid white lines, allowing CDW and FFLO order to form with nesting vector $\vec{Q}$.

of arcs on the same or different surfaces, yielding multiple ways in which these kinds of orders set in. As we shall see, while these orderings coexist, they also compete, leading to quantum phase transitions among different realizations of the broken symmetries with variations of the system parameters.

Associated with these broken symmetry states are Goldstone modes. The broken translational symmetry characteristic of CDW order leads to phonon modes, which at zero wavevector becomes a sliding mode that is generically pinned by disorder [33]. Exciton condensation yields gapless superfluid modes [34–37] which in such double layer systems is realized as a dissipationless counterflow current. Moreover, very weak tunneling between surfaces may yield Josephson-like transport behavior between them [38, 39]. Such collective behavior can be observed in a variety of transport experiments [39–43].

As a paradigm of such systems, we consider a setup of two capacitively coupled WSM surfaces, each host-

ing FAs (see Fig. 1). For simplicity we consider straight arcs, although our qualitative results do not depend significantly on this simplification [see Supplementary Material (SM) [44]]. We find that electron-hole coherence may develop among some or all of the arcs, depending on their relative angles and interaction strengths. For arcs on different surfaces with common in-plane wavevectors, strong interlayer coherence can develop at these common wavevectors [29]. Interlayer coherence can also develop between arcs on different surfaces whose wavevectors are remote from one another, and surprisingly these coherences can be stronger than the direct case, particularly when the the arcs are nested. Such finite momentum interlayer ordering may be understood as an exciton condensate analog of the Fulde-Ferrell-Larkin-Ovchinikov (FFLO) superconductor. We find that these direct exciton (D-ex) and "FFLO exciton" (FFLO-ex) orderings are often both present, but tend to compete, so that as one type of ordering increases the other shrinks. With both present, the interlayer coherence should have spatial oscillations in real space. In addition to this, intra-layer coherence between arcs on the same surface yields CDW order.

When CDW and exciton orders coexist, the system is in a supersolid state [45]. Such order has been considered for bilayer systems in which Wigner crystals may form at low electron density [46–48], and tends to be associated with excitons localizing at sites in a two-dimensional crystal. By contrast, in the coupled WSM surface system, the spatial ordering is determined by nesting vectors rather than by carrier density, so that there is no strong locking of the average inter-exciton separation with the CDW period. Thus we expect the superfluid ordering to be more robust with respect to disorder than for the bilayer Wigner crystal system. A unique feature of the coupled FA system is the possibility of manipulating the relative strength of the spontaneous orderings by modifying the twist angle between surfaces, giving this system a level of tunability not present in more traditional materials. The presence of multiple continuously broken symmetries in this system implies that their superfluid modes will be coupled, so that counterflow superfluidity may become admixed with CDW sliding. This could yield threshold behavior in counterflow supercurrent, above which narrow band noise is sustained. Detection of such phenomenology associated with both exciton and CDW condensation would constitute direct evidence that the system hosts supersolid order.

Model– For concreteness, we consider a system of two WSMs with parallel surfaces labeled by an index $\eta = \pm 1$, a distance t apart, with each surface hosting two FAs labeled by an index $\xi = \pm 1$, in general not parallel to one another [Fig. 2(a)]. Each FA joins the projections of two Weyl nodes onto the surface Brillouin-zone, with wave functions that decay exponentially in the bulk of the WSM. The associated decay length diverges at the
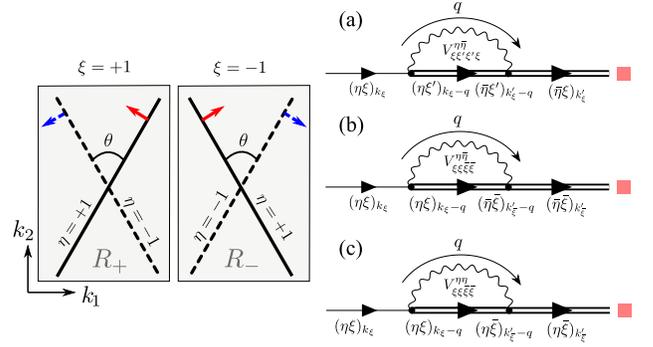
FIG. 2. Left: Configurations of the FAs where solid and the dashed lines denote the states on the two surfaces ($\eta = \pm 1$). $\xi = \pm 1$ are two FAs on the same surface, at momentum region R_ξ. Directions of dispersions are marked by arrows. Pairs of FAs with $\xi \eta = \pm 1$ are nested with momentum $\vec{Q}$, which disperse in opposite directions. Right: Self-energy diagrams which describe spontaneously broken symmetries. k_ξ, q represent four vectors, with momenta $\vec{k}_\xi \in R_\xi$. (a), (b) and (c) gives rise to self-energies for D-ex , FFLO-ex and CDW orders, respectively. ▪ stands for any of (η, ξ).

Weyl node projections, which we model by the inverse of a mass function $M_\xi(\vec{k})$ [49]. The single-particle energy associated with each arc has the form $\epsilon_\xi(\vec{k}) = \pm \hbar v_F k_\perp^\xi$, which disperses with the momentum component perpendicular to the ark, $k_\perp^\xi$. Note the sign of this dispersion characterizes the helicity of the FA. Further details of the model are provided in the SM [44].

We model interactions among the electrons by

$$H_{\text{int}} = \sum_{\eta\eta'} \int_{\vec{r},\vec{r}'} V^{\eta\eta'}(\vec{r} - \vec{r}') : \hat{\rho}^\eta(\vec{r})\hat{\rho}^{\eta'}(\vec{r}') :, \quad (1)$$

where $\hat{\rho}^\eta = \sum_{\xi\xi'} \hat{\Psi}_\xi^{\eta\dagger}\hat{\Psi}_{\xi'}^\eta$, with $\hat{\Psi}_\xi^\eta$ being the field operator of the (η, ξ) FA. The functions $V^{++} = V^{--}$ and $V^{+-} = V^{-+}$ are the intra- and inter-surface Coulomb interactions, respectively [44]. The decay depth of the single particle states entering our decomposition of the field operators $\hat{\Psi}_\xi^\eta$ impacts the matrix elements appearing when Eq. (1) is written in terms of the non-interacting FA states; beyond this, our model is two-dimensional. We do not explicitly include bulk states in our analysis, although they can be approximately accounted for via screening in the interactions.

Green's Function and Broken Symmetry States – With these simplifications, components of the non-interacting finite-temperature Green's function of the WSM surfaces are given by $\mathcal{G}_{ij}^0(\vec{k}, i\omega_n) = \delta_{ij}/(i\omega_n - \epsilon_i(\vec{k}))$, where $\omega_n = (2n + 1)/k_B T$ are the fermionic Matsubara frequencies at temperature T and the i, j subscripts are composite indices for η and ξ. To describe the broken symmetry states, we include interactions through a self-energy matrix Σ, which introduces components in the Green's function even for $i \neq j$, as well as between different wave-vectors. These encode spontaneous ordering

between different flavors of the fermions as well as possible translation symmetry breaking. We summarize the important diagrammatic terms that appear, within the non-crossing approximation [50, 51], in Fig. 2(b).

In general, the full Green's function $\mathcal{G}$, non-interacting Green's function $\mathcal{G}^0$, and self-energy are related by the Dyson equation, to be solved self-consistently, $\mathcal{G} = \mathcal{G}^0 + \mathcal{G}^0 \Sigma \mathcal{G}$. The diagrams illustrated in Fig. 2(b) represent the last term in this equation. Numerical solution of these requires integration over momentum, which we approximate as a discrete sum over limited regions (denoted by R_ξ in Fig. 2(a)) of the surface Brillouin zone in the vicinities of the FA's. In addition there is a Mastubara frequency sum, and the resulting self-energies are then independent of frequency because our model interaction is frequency independent. Further details of our numerical scheme are in the SM [44].

Denoting $\bar{\eta} = -\eta$ and $\bar{\xi} = -\xi$, and k_ξ for the 3-momentum $(\vec{k}_\xi, \omega_n)$, we group the self-energies into three classes. Coherence between FA's on different surfaces that do not spontaneously break translation symmetry have the form $\Sigma_{\xi\bar{\xi}}^{\eta\bar{\eta}}(k_\xi, k_\xi')$, and represent direct exciton order (D-ex) [23]. In addition, coherence between FA's on different surfaces which are separated in wavevector can also form, breaking both the gauge symmetry associated with individual layers and translational symmetry spontaneously, resulting in FFLO-ex order. Such ordering is encoded in self-energy terms of the form $\Sigma_{\xi\bar{\xi}}^{\eta\bar{\eta}}(k_\xi, k_{\bar{\xi}}')$. Finally, intra-layer interactions also give rise to self-energies of the form $\Sigma_{\xi\bar{\xi}}^{\eta\eta}(k_\xi, k_{\bar{\xi}}')$, which indicate CDW order within a surface. For simplicity, we neglect the diagonal terms in the self-energy $\Sigma_{\xi\xi}^{\eta\eta}$, which are expected to simply renormalize the non-interacting FA velocities.

Before we discuss our numerical results, several comments are in order. Firstly, for the particular FA orientations shown in Fig. 1, some FAs have parallel sections with nesting momentum $\vec{Q}$. Particularly for the FFLO-ex order, one expects the dominant contribution of $\Sigma_{\xi\bar{\xi}}^{\eta\bar{\eta}}(\vec{k}_\xi, \vec{k}_{\bar{\xi}}')$ to occur at

$$\vec{k}_\xi - \vec{k}_{\bar{\xi}}' = \pm\vec{Q}. \tag{2}$$

Our numerical findings verify this for both FFLO-ex and CDW orders. Numerical calculations can be greatly simplified by assuming these self-energies vanish except at this momentum difference. We have compared this to results where the momentum difference is unconstrained in a few representative cases, and find rather good agreement [44]. Secondly, we characterize the strength of this Coulomb interaction by an effective fine-structure constant, $\alpha = (c/\varepsilon v_F)/137$. Unless otherwise specified, we assume $\alpha = 5/\varepsilon$, which is consistent with $v_F \sim 10^5$m/s. For the intra-surface interaction we adopt a dielectric constant $\varepsilon = 4$, while for the inter-surface interaction it is fixed at unity. We make the wave-vectors and lengths unitless in terms of a lattice-spacing distance (a_0) and we
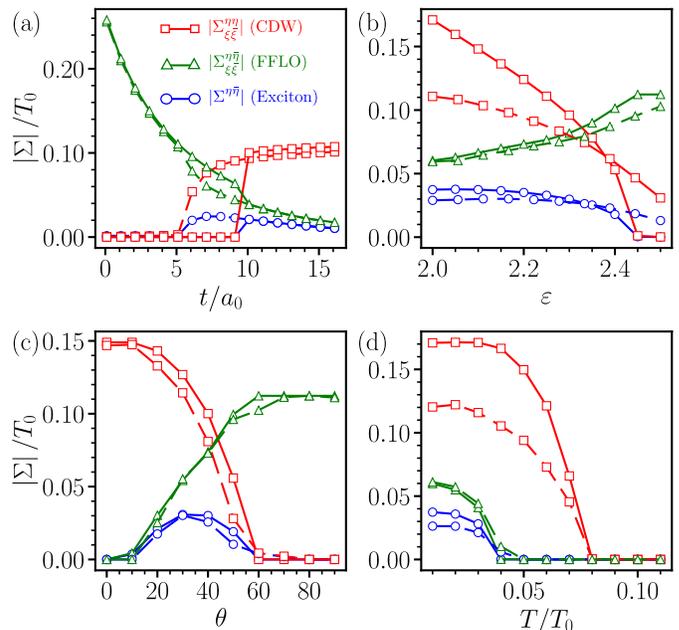
FIG. 3. Behavior of maximum order parameter magnitudes with system parameters. Variation with: (a) surface separation (t); (b) WSM dielectric constant (ε); (c) FA tilt angle (θ). Solid lines represent numerical results where the constraint Eq. (2) is enforced. Results marked by dashed lines have these constraints relaxed. (d) Critical temperatures of the three order parameters, in units of T_0 (see main text). $\theta = 60°$ is used in (a), (b) and (d). Other parameters: for (a), $\varepsilon = 2$; for (b), $t/a_0 = 5$; for (c), $t/a_0 = 5, \varepsilon = 2.5$; for (d), $t/a_0 = 5, \varepsilon = 2$. The separation of the Weyl nodes, as well as the nesting vector $|\vec{Q}|$, is taken to be 0.4Å^{-1}.

consider the unit of our energy-scale to be $T_0 = \hbar v_F/a_0$. With $a_0 \sim 5\text{Å}$, we have T_0 of the order of 10^3K.

Competing phases– The numerical results we obtain indicate an intricate competition among the order parameters discussed above. Some typical results are illustrated in Fig. 3. At large t, for which interactions between surfaces are weak, intra-layer CDW order dominates, while for smaller separation and stronger inter-surface coupling, we find the FFLO-ex order dominates the CDW order. The competition between them is clearly visible in Figs. 3(a) and (b), in which we vary the separation between layers, and hence the relative intra- and inter-layer interactions. Interestingly, at small separation only the FFLO-ex order is present, but with increasing separation a transition occurs in which D-ex and CDW orders set in, accompanied by a sharp drop in the FFLO-ex order. This demonstrates the competition among the different types of order the system supports. Note that for much of the parameter regime, the simplifying assumption expressed in Eq. (2) yields results largely consistent with calculations where this constraint is relaxed, except in the transition region, where it is necessary to relax the constraint to correctly capture its second order nature.

For fixed separation, it is notable that increasing the tilt angle between the arcs tends to enhance the FFLO-ex order at the expense of the D-ex and CDW orders, as shown in Fig. 3(c). This is clearly a consequence of the strong nesting between the arcs involved in the FFLO-ex ordering, which persists at all angles. The relatively stronger stability of the this ordering is also apparent in the temperature dependence of the order parameters, illustrated in Fig. 3(d), indicating different critical temperatures for FFLO-ex and CDW orders. Interestingly we find that the critical temperature of the direct exciton order coincides with that of the intra-layer CDW order. At low temperatures, all three orders may coexist, and with rising temperature a transition may take place from such a *multiply-ordered phase* to a phase with only FFLO-ex order. This intricate interplay of competition and cooperation among the different possible broken symmetries is one of the central results of this work.

Note that the FA dispersions shown in the Fig. 2(a) are oriented so that nested FAs of opposite surfaces disperse in opposite directions. This supports the FFLO-ex order. One may also consider situations in which they disperse in the *same* direction. This could occur, for example, in WSM's with bulk magnetizations with opposite orientations. This results in the loss of FFLO-ex order. Introduction of curvature in the FA's also tends to suppress this order, although does not eliminate it (see SM [44].)

Goldstone modes and counterflow currents– Our model system involves four flavors of fermions (specified by η and ξ), and each has an individually conserved charge that is encoded by a $U(1)$ symmetry. The mean-field ground states we find spontaneously break at most three of these symmetries, so that all our phases respect global charge conservation. Although in general the six self-energy terms ($\Sigma_{\xi\xi'}^{\eta\eta'}$, excluding $\xi = \xi'$ and $\eta = \eta'$) may attain non-zero values, their phases, $\theta_{\xi\xi'}^{\eta\eta'}$, are not independent. A close examination of the equations for the self-energies reveals the relations, $\theta_{\xi\xi}^{+-} + \theta_{\bar{\xi}\bar{\xi}}^{++} = n_1\pi$, $\theta_{\xi\xi}^{+-} + \theta_{\xi\bar{\xi}}^{-+} = n_2\pi$, $\theta_{-+}^{\eta\bar{\eta}} + \theta_{+-}^{\eta\eta} = n_3\pi$, where repeated indices are summed and the n_i's may be 0 or ± 1 depending on the parameters. Fluctuations of the phases that violate the above relations are massive, but variations which keep these relations intact increase the energy of the system only when they have spatial or temporal gradients. Thus we expect our system to support three gapless Goldstone modes. As detailed in the SM [44], one may formally derive an effective action for phase fluctuations valid for small gradients in terms of three independent phases, θ_i ($i = 1, 2, 3$), $S[\{\theta_i\}] \approx \sum_q \sum_{m,n} \Pi_{mn}(q)\theta_n(q)\theta_m(-q)$, where $\Pi_{nm}(q)$ is the polarizability function. The normal modes of S represent gapless modes, $\tilde{\theta}_i$, which are linear combinations of θ_i. Static spatial gradients in these phases generally represent supercurrents, $(j_\xi^\eta)_l = \sum_{i=1,2,3} \Gamma_{\eta\xi i}^l \nabla_l \tilde{\theta}_i$. We

present details of the form of Γ for a simplified model in the SM [44]; in general it depends on details of the system parameters and broken symmetries encoded in the Σ matrix. The entangling of different types of supercurrents, usually associated with interlayer counterflow currents [39] or sliding CDW modes [33], is an important signature that in the generic case the ground state of this system is a *supersolid*. Remarkably, for inversion-symmetric cases, we find a sum rule, $\sum_{\xi\eta}(j_\xi^\eta)_l = 0$, indicating that the system does not support charged supercurrents. While natural for particle-hole condensates, which support counterflow supercurrents, this is less obvious for CDW dynamics which support sliding modes. We discuss the implications of this below.

Discussion and Summary– We have demonstrated that parallel surfaces of WSM's, with each hosting multiple FAs, in general support broken symmetries within and between the surfaces. In particular, we show FFLO-exciton order may completely suppress direct-exciton and CDW orders, or may coexist with them. In the latter case the system is a supersolid. The entangling of orders in such a system is evidenced by its Goldstone modes, which in general have mixed counterflow - sliding CDW characters. In real systems, sliding behavior of CDW's are not observed as a dissipationless current, because their broken translational symmetry necessary implies they will become pinned by disorder. Nevertheless, they host unique transport signatures: threshold driving fields above which the a CDW may depin, and narrow-band noise with frequency proportional to the current above threshold [33]. An interesting signature of the supersolid character of this system would be the observation of these signatures in a counterflow experiment.

Several materials represent potential candidates for the physics described in this study. These include spinel compounds (such as VMg$_2$O$_4$) [52] and cobalt-based semimetals (such as Co$_3$Sn$_2$S$_2$). The former has two FAs on (110) surfaces, which are non-colinear and may serve as potential hosts for the physics we describe. For certain surface terminations, Co$_3$Sn$_2$S$_2$ has three FAs which are oriented at 120º angle with each other. For two such surfaces oriented at $\sim 180°$ one will have four FAs in approximately the configuration we consider; the other two may support their own FFLO-exciton condensation, but will essentially decouple from the other four FA's (see SM [44]).

For simplifications of the numerical analysis, we considered straight FAs for the non-interacting WSM surfaces. As argued in the Ref. 29, in presence of a curvature in the FAs, there is an associated first order phase-transition with increasing curvature of the FAs. A full solution for the interacting Green's function in this case is numerically challenging; some results are presented in the SM [44]. Moreover, in our idealization of these systems we have ignored the presence of bulk states which may be present at the Fermi energy, and can have fi-

nite support at the surfaces. Their impact on the broken symmetry states and associated supercurrents are interesting subjects for further study of these remarkably rich systems.

---

[1] For reviews see: N. P. Armitage, E. J. Mele, and A. Vishwanath, Rev. Mod. Phys. **90**, 015001 (2018); Nature S. Jia, S.-Y. Xu, and M. Z. Hasan, Nature Materials **15**, 1140–1144 (2016); S. Rao, Journal of the Indian Institute of Science, **96**, 2 (2016).

[2] E.V. Gorbar, V.A. Miransky, I.A. Shovkovy, and P.O. Sukhachov, *Electronic Properties of Dirac and Weyl Semimetals*, (World Scientific, Singapore, 2021).

[3] B. Q. Lv, H. M. Weng, B. B. Fu, X. P. Wang, H. Miao, J. Ma, P. Richard, X. C. Huang, L. X. Zhao, G. F. Chen, Z. Fang, X. Dai, T. Qian, and H. Ding, Phys. Rev. X **5**, 031013 (2015).

[4] Zhang C, Ni Z, Zhang J, Yuan X, Liu Y, Zou Y, Liao Z, Du Y, Narayan A, Zhang H, Gu T, Zhu X, Pi L, Sanvito S, Han X, Zou J, Shi Y, Wan X, Savrasov SY, Xiu F., Nat. Mater. 18, 482–488 (2019).

[5] Zhicheng Rao, Hang Li, Tiantian Zhang, Shangjie Tian, Chenghe Li, Binbin Fu, Cenyao Tang, Le Wang, Zhilin Li, Wenhui Fan, Jiajun Li, Yaobo Huang, Zhehong Liu, Youwen Long, Chen Fang, Hongming Weng, Youguo Shi, Hechang Lei, Yujie Sun, Tian Qian, and Hong Ding, Nature **567**, 496–499 (2019).

[6] Guowei Li, Qiunan Xu, Wujun Shi, Chenguang Fu, Lin Jiao, Machteld E. Kamminga, Mingquan Yu, Harun Tüysüz, Nitesh Kumar, Vicky Süß, Rana Saha, Abhay K. Srivastava, Steffen Wirth, Gudrun Auffermann, Johannes Gooth, Stuart Parkin, Yan Sun, Enke Liu, Claudia Felser, Science Advances Vol. 5, no. 8 (2019).

[7] M. Tanaka, Y. Fujishiro, M. Mogi, Y. Kaneko, T. Yokosawa, N. Kanazawa, S. Minami, T. Koretsune, R. Arita, S. Tarucha, M. Yamamoto, and Y. Tokura, Nano Lett. 2020, 20, 10, 7476–7481.

[8] Hemian Yi, Zhijun Wang, Chaoyu Chen, Youguo Shi, Ya Feng, Aiji Liang, Zhuojin Xie, Shaolong He, Junfeng He, Yingying Peng, Xu Liu, Yan Liu, Lin Zhao, Guodong Liu, Xiaoli Dong, Jun Zhang, M. Nakatake, M. Arita, K. Shimada, H. Namatame, M. Taniguchi, Zuyan Xu, Chuangtian Chen, Xi Dai, Zhong Fang, and X. J. Zhou, Scientific Reports volume **4**, 6106 (2014).

[9] Su-Yang Xu, Nasser Alidoust, Ilya Belopolski, Zhujun Yuan, Guang Bian, Tay-Rong Chang, Hao Zheng, Vladimir N. Strocov, Daniel S. Sanchez, Guoqing Chang, Chenglong Zhang, Daixiang Mou, Yun Wu, Lunan Huang, Chi-Cheng Lee, Shin-Ming Huang, BaoKai Wang, Arun Bansil, Horng-Tay Jeng, Titus Neupert, Adam Kaminski, Hsin Lin, Shuang Jia, and M. Zahid Hasan, Nature Physics **11**, pages 748–754 (2015).

[10] Mehdi Kargarian and Mohit Randeria, and Yuan-Ming Lu, M. Kargarian, M. Randeria, and Y.-M. Lu, Proc. Natl. Acad. Sci. U.S.A. **113**, 8648 (2016).

[11] Philip J. W. Moll, Nityan L. Nair, Toni Helm, Andrew C. Potter, Itamar Kimchi, Ashvin Vishwanath, and James G. Analytis, Nature **535**, pages 266–270 (2016).

[12] Yun Wu, Na Hyun Jo, Lin-Lin Wang, Connor A. Schmidt, Kathryn M. Neilson, Benjamin Schrunk, Przemyslaw Swatek, Andrew Eaton, S. L. Bud'ko, P. C. Canfield, and Adam Kaminski, Phys. Rev. B **99**, 161113(R), (2019).

[13] Cai-Zhen Li, An-Qi Wang, Chuan Li, Wen-Zhuang Zheng, Alexander Brinkman, Da-Peng Yu, and Zhi-Min Liao, Nature Communications **11**, 1150 (2020).

[14] Johannes Hofmann and Sankar Das Sarma, Phys. Rev. B **93**, 241402(R) (2016).

[15] Gian Marcello Andolina, Francesco M. D. Pellegrino, Frank H. L. Koppens, and Marco Polini, Phys. Rev. B **97**, 125431 (2018).

[16] Gennaro Chiarello, Johannes Hofmann, Zhilin Li, Vito Fabio, Liwei Guo, Xiaolong Chen, Sankar Das Sarma, and Antonio Politano, Phys. Rev. B **99**, 121401(R) (2019).

[17] E. V. Gorbar, V. A. Miransky, I. A. Shovkovy, and P. O. Sukhachov, Phys. Rev. B **99**, 155120 (2019).

[18] Kota Tsuchikawa, Satoru Konabe, Takahiro Yamamoto, and Shiro Kawabata, Phys. Rev. B 102, 035443 (2020).

[19] Justin C. W. Song and Mark S. Rudner, Phys. Rev. **B** 96, 205443 (2017).

[20] Zeljana Bonacic Losic, J. Phys.: Condens. Matter **30**, 365003 (2018).

[21] Tomohiro Tamaya, Takeo Kato, Satoru Konabe, and Shiro Kawabata, J. Phys.: Condens. Matter **31**, 305001 (2019).

[22] S. Oskoui Abdol, A. Soltani Vala, and B. Abdollahipour, J. Phys.: Condens. Matter **31** (2019).

[23] Sayandip Ghosh and Carsten Timm, Phys. Rev. B **101**, 165402 (2020).

[24] H. Wei, S.-P. Chao, and V. Aji, Phys. Rev. Lett. **109**, 196403 (2012).

[25] M. Laubach, C. Platt, R. Thomale, T. Neupert, and S. Rachel, Phys. Rev. B **94**, 241102(R) (2016).

[26] V. Dwivedi, Phys. Rev. B **97**, 064201 (2018).

[27] Ganpathy Murthy, H.A. Fertig, and Efrat Shimshoni, Phys. Rev. Research **2**, 013367 (2020)

[28] Faruk Abdulla, Sumathi Rao, and Ganpathy Murthy, Phys. Rev. B **103** 235308 (2021).

[29] Paolo Michetti and Carsten Timm, Phys. Rev. B **95**, 125435 (2017).

[30] C.-H. Zhang and Yogesh N. Joglekar, Phys. Rev. B **77**, 233405 (2008).

[31] Maxim Yu. Kharitonov and Konstantin B. Efetov, Phys. Rev. B **78**, 241401(R) (2008).

[32] D. S. L. Abergel, R. Sensarma, and S. Das Sarma, Phys. Rev. B **86**, 161412(R)(2012).

[33] G. Gruner, Rev. Mod. Phys. **60**, 1129 (1988).

[34] D. Snoke, Science **298**, 1368 (2002).

[35] Hongki Min, Rafi Bistritzer, Jung-Jung Su, and A. H. MacDonald, Phys. Rev. B 78, 121401(R) (2008).

[36] M.M. Fogler, L.V. Butov, and K.S. Novoselov, Nat. Commun. **5**, 4555 (2014).

[37] M. Combescot, R. Combescot, and F. Dubin, Rep. Prog. Phys. **80**, 066501 (2017).

[38] Fabrizio Dolcini, Diego Rainis, Fabio Taddei, Marco Polini, Rosario Fazio, and A. H. MacDonald, Phys. Rev. Lett. **104**, 027004 (2010).

[39] J. Eisenstein, Annual Review of Condensed Matter Physics **5**, 159-181 (2014).

[40] J.-J. Su and A. H. MacDonald, Nat. Phys. **4**, 799 (2008).

[41] A. V. Balatsky, Y. N. Joglekar, and P. B. Littlewood, Phys. Rev. Lett. **93**, 266801 (2004).

[42] M. P. Mink, H. T. C. Stoof, R. A. Duine, Marco Polini, and G. Vignale, Phys. Rev. Lett. **108**, 186402 (2012).

[43] J. A. Seamons, C. P. Morath, J. L. Reno, and M. P. Lilly, Phys. Rev. Lett. 102, 026804 (2009).

[44] See Supplementary Material, where we discuss (i) theoretical details of the dispersions of multiple Fermi-arcs (FA) that we consider, (ii) Coulomb matrix elements, scattering vertices and the construction of self-energies for solving the interacting Green's function, (iii) variation of the self-energy amplitudes with system parameters, (iv) action of phase fluctuations and the condition of counter-flow currents on the FAs, and (v) the case of three FA system.

[45] Massimo Boninsegni and Nikolay V. Prokof'ev, Rev. Mod. Phys. **84**, 759 (2012).

[46] Yogesh N. Joglekar, Alexander V. Balatsky, and S. Das Sarma Phys. Rev. B **74**, 233302 (2006).

[47] L. Zheng and H.A. Fertig, Phys. Rev. B **52**, 12282 (1995).

[48] Subha Narasimhan and Tin-Lun Ho, Phys. Rev. B **52**, 12291 (1995).

[49] Sonu Verma, Debasmita Giri, H.A. Fertig, and Arijit Kundu, Phys. Rev. B **101**, 085419 (2020).

[50] Altland, A., & Simons, B. (2010). Condensed Matter Field Theory (2nd ed.). Cambridge: Cambridge University Press. doi:10.1017/CBO9780511789984.

[51] Giuliani, G., & Vignale, G. (2005). Quantum Theory of the Electron Liquid. Cambridge: Cambridge University Press. doi:10.1017/CBO9780511619915

[52] Wei Jiang, Huaqing Huang, Feng Liu, Jian-Ping Wang, and Tony Low, Phys. Rev. B **101**, 121113(R) (2020).